CD27-CD70 Costimulation Controls T Cell Immunity during Acute and Persistent Cytomegalovirus Infection

Suzanne P. M. Welten,[a] Anke Redeker,[a] Kees L. Franken,[a] Chris A. Benedict,[b] Hideo Yagita,[c] Felix M. Wensveen,[d] Jannie Borst,[e] Cornelis J. M. Melief,[a,f] René A. W. van Lier,[e] Klaas P. J. M. van Gisbergen,[e] Ramon Arens[a]

Department of Immunohematology and Blood Transfusion, Leiden University Medical Center, Leiden, The Netherlands[a]; Division of Immune Regulation, La Jolla Institute for Allergy and Immunology, La Jolla, California, USA[b]; Department of Immunology, Juntendo University School of Medicine, Tokyo, Japan[c]; Department of Hematopoiesis, Sanquin Research at Central Laboratory of the Blood Transfusion Service and Landsteiner Laboratory, Amsterdam, The Netherlands[d]; Division of Immunology, The Netherlands Cancer Institute, Amsterdam, The Netherlands[e]; ISA Therapeutics, Leiden, The Netherlands[f]

Cytomegaloviruses (CMVs) establish lifelong infections that are controlled in part by CD4$^+$ and CD8$^+$ T cells. To promote persistence, CMVs utilize multiple strategies to evade host immunity, including modulation of costimulatory molecules on infected antigen-presenting cells. In humans, CMV-specific memory T cells are characterized by the loss of CD27 expression, which suggests a critical role of the costimulatory receptor-ligand pair CD27-CD70 for the development of CMV-specific T cell immunity. In this study, the *in vivo* role of CD27-CD70 costimulation during mouse CMV infection was examined. During the acute phase of infection, the magnitudes of CMV-specific CD4$^+$ and CD8$^+$ T cell responses were decreased in mice with abrogated CD27-CD70 costimulation. Moreover, the accumulation of inflationary memory T cells during the persistent phase of infection and the ability to undergo secondary expansion required CD27-CD70 interactions. The downmodulation of CD27 expression, however, which occurs gradually and exclusively on inflationary memory T cells, is ligand independent. Furthermore, the IL-2 production in both noninflationary and inflationary CMV-specific T cells was dependent on CD27-CD70 costimulation. Collectively, these results highlight the importance of the CD27-CD70 costimulation pathway for the development of CMV-specific T cell immunity during acute and persistent infection.

During the millions of years of coevolution with their vertebrate hosts, cytomegaloviruses (CMVs), members of the betaherpesvirus family, have developed numerous viral immune evasion mechanisms to promote their lifelong persistence (1, 2). The successful adaption of CMV is exemplified by the universal presence of human cytomegalovirus (HCMV) in the world's population (3). Although HCMV infection is generally asymptomatic and harmless in healthy individuals, it can become life threatening in cases of developmental or acquired immune deficits. In particular, primary CMV infection during pregnancy can result in congenital infection of the infant, with severe neurological sequelae (4). Furthermore, severe HCMV-associated disease oftentimes develops in HIV-infected patients, CMV-seronegative individuals who receive organ transplants from CMV-seropositive donors, and recipients of CMV-infected allogeneic bone marrow (5).

Clinical investigations and findings in experimental models of CMV, such as mouse CMV (MCMV) and rhesus macaque CMV (rhCMV), have established a critical role for CD4$^+$ and CD8$^+$ T cells in the control of CMV infection. Whereas CMV-specific CD4$^+$ T cells are particularly important during the primary phase of infection to control viral replication, CD8$^+$ T cells are instrumental during reactivation of the virus and confer superior protection during reexposure (6–11). Moreover, immunotherapy with CMV-specific T cells offers the best protection when both CD4$^+$ and CD8$^+$ T cells are adoptively transferred (5, 12). Upon CMV infection, a heterogeneous CD8$^+$ T cell response develops, and during the acute and persistent phases of CMV infection, CD8$^+$ T cells with dissimilar characteristics prevail (13, 14). CD8$^+$ T cells that develop into central memory-like (CD127$^+$ CD62L$^+$ KLRG1$^-$ IL-2$^+$) cells undergo expansion during acute CMV infection, followed by contraction and stable maintenance at low frequencies. During the persistent phase of infection, CD8$^+$ T cells

specific for certain CMV epitopes increase in frequency and are maintained at high levels throughout infection. The T cells that undergo this so-called memory T cell inflation are characterized by an effector memory phenotype (CD127$^-$ CD62L$^-$ KLRG1$^+$ IL-2$^{+/-}$) (15). Memory inflation has also been observed for CMV-specific CD4$^+$ T cells (16). Due to the induction of large numbers of functional effector memory T cells, CMV is an interesting candidate to explore as a vaccine platform for chronic viral infections and cancer (15). The factors that control the inflationary T cell pool are only beginning to be understood, and understanding such factors is pivotal for further exploiting CMV-based vaccines.

The loss of the costimulatory receptor CD27 on circulating T cells seems to be associated uniquely with HCMV infection in comparison with other (persistent) viral infections (17–20), and it is particularly related to inflationary rather than noninflationary T cells (13, 21). Furthermore, *in vitro* studies indicated that CD70, the only known ligand for CD27, might be a key regulator in determining the size and phenotype of the CMV-specific T cell pool (19). However, the physiological role of the costimulatory receptor-ligand pair CD27-CD70 during CMV infection is unclear. Here we determined the *in vivo* role of CD27-CD70 costimulation in a murine CMV model and found that the development of both noninflationary and inflationary memory T cell responses, as well as the ability to undergo secondary memory

expansion and autocrine interleukin-2 (IL-2) production, is highly dependent on this costimulatory receptor-ligand pair. These results highlight the importance of CD27-CD70 costimulation as a key molecular interaction in the development of T cell immunity to CMV.

MATERIALS AND METHODS

Mice. C57BL/6 mice were purchased from Charles River (L'Arbresle, France) and were used as wild-type (WT) mice. Ovalbumin-specific T cell receptor (TCR) transgenic OT-I mice and the congenic strains Thy1.1 (CD90.1) and Ly5.1 (SJL; CD45.1), all on a C57BL/6 background, were obtained from The Jackson Laboratory. CD27$^{-/-}$ mice were made on a 129/Ola background and backcrossed for 8 generations to a C57BL/6 background (22). CD70$^{Cre/Cre}$ mice, in which CD70 expression is lost due to replacement of exon 1 of the CD70 gene with the Cre recombinase coding sequence, were generated as described previously, on a 129/Ola background, and backcrossed by speed congenics to a C57BL/6 background (23). Mice were maintained under specific-pathogen-free conditions at the Central Animal Facility of the Leiden University Medical Center and were 8 to 12 weeks of age at the start of each experiment. All animal experiments were approved by the Animal Experiments Committee of the Leiden University Medical Center and were performed according to the guide to animal experimentation set by the Leiden University Medical Center and to the Dutch Experiments on Animals Act, which serves to implement the *Guidelines on the Protection of Experimental Animals* by the Council of Europe (24).

Virus preparation, quantification, and infection. MCMV-Smith (VR-194) was obtained from the American Type Culture Collection (Manassas, VA), and this wild-type virus was prepared from the salivary glands of infected BALB/c mice as described previously (25). MCMV-Δm157 has been described previously (26) and is derived from the MCMV bacterial artificial chromosome (BAC) pSM3fr. MCMV-OVA was obtained from Geoffrey R. Shellam (School of Biomedical, Biomolecular and Chemical Sciences, Crawley, Western Australia, Australia). Stocks of the viral recombinants (MCMV-Δm157 and MCMV-OVA) were propagated in NIH 3T3 cells and were prepared as reported previously (25). Gender- and age-matched mice were infected intraperitoneally (i.p.) with 1×10^4 or 5×10^4 PFU of salivary gland-derived MCMV-Smith, 1×10^4 PFU of MCMV-Δm157, or 5×10^5 PFU of MCMV-OVA. Viral titers of virus stocks or infected tissues were determined by plaque assays. In short, serial dilutions of virus stocks or organ homogenates were added to monolayers of NIH 3T3 cells in 12-well dishes. The monolayers with virus stocks were incubated for 1 h at 37°C, and the monolayers with organ homogenates were incubated for 5 min at 37°C followed by centrifugation at $400 \times g$ for 10 min and an additional 5 min of incubation at 37°C. After incubation, inoculums were removed and cells were covered in 5% carboxymethyl cellulose-containing medium. After 5 days, the monolayers were washed, fixed, and stained with crystal violet solution to visualize plaques.

Lymphocytic choriomeningitis virus (LCMV) Armstrong and clone 13, obtained from Shane Crotty (La Jolla Institute for Allergy and Immunology, La Jolla, CA), were propagated in BHK cells, and the titers were determined by plaque assays on Vero cells as described previously (27). For acute LCMV infection, mice were infected i.p. with 2×10^5 PFU LCMV Armstrong. For chronic LCMV infection, mice were infected intravenously (i.v.) via retro-orbital injection with 2×10^6 PFU LCMV clone 13.

***In vivo* antibody treatment.** Hybridomas were cultured in Life Technologies protein-free hybridoma medium II (Invitrogen), and monoclonal antibodies were purified using protein G columns. For *in vivo* antibody treatment during the acute phase of MCMV infection, 150 μg of anti-mouse CD70 antibody (clone FR70) or control rat IgG was administered on days −1, 0, and 3 postinfection. For CD70 blocking over a prolonged period, mice received 150 μg anti-CD70 antibody or control IgG once every 3 days. No signs of serum sickness (immune complex hypersensitivity) were observed during long-term antibody treatment. Serum levels of FR70 were detected by an enzyme-linked immunosorbent assay (ELISA) using purified polyclonal and biotin-labeled anti-rat antibodies (BD Pharmingen). To deplete CD4$^+$ T cells, mice received 200 μg anti-mouse CD4 antibody (clone GK1.5) on days −1, 0, and 3 after infection. To deplete CD8$^+$ T cells, mice received 200 μg anti-mouse CD8 antibody (clone 2.43) on days 3 and 5 postinfection. For depletion of CD8$^+$ T cells prior to adoptive transfer, mice received 75 μg anti-CD8 antibodies on day −7. All antibodies were administered in 400 μl phosphate-buffered saline (PBS) by i.p. injection.

Flow cytometry. Single-cell suspensions were prepared from spleens by mincing the tissue through a 70-μm cell strainer (BD Biosciences). Erythrocytes were lysed in a hypotonic ammonium chloride buffer. Before livers and lungs were removed, mice were perfused with PBS containing EDTA to remove all blood-associated lymphocytes. Lymphocytes were isolated from these organs by collagenase and DNase treatment for 0.5 h, followed by Percoll gradient centrifugation. The magnitudes and characteristics of the MCMV-specific T cell responses were determined by major histocompatibility complex (MHC) class I tetramer staining and/or intracellular cytokine staining as described elsewhere (28, 29). Conjugated monoclonal antibodies to mouse CD3 (V500), CD4 (phycoerythrin [PE]-Cy7), CD4 (Qdot-605), CD8 (Alexa 700), CD8 (peridinin chlorophyll protein [PerCp]-Cy5.5), CD25 (fluorescein isothiocyanate [FITC]), CD27 (FITC), CD44 (eFluor450), CD45.1 (eFluor450), CD45.2 (eFluor780), CD62L (eFluor450), CD62L (eFluor780), CD69 (eFluor450), CD90.1 (PerCp), CD90.2 (PE-Cy7), CD127 (biotin), CXCR3 (PE), DX5 (PE), gamma interferon (IFN-γ) (allophycocyanin [APC]), IL-2 (PE), KLRG-1 (PE-Cy7), Ly49H (APC), NK1.1 (APC-Cy7), PD-1 (PE), tumor necrosis factor (TNF) (FITC), and Vα2 (PE) were purchased from eBioscience or BD Biosciences. Streptavidin-PE (eBioscience) was used to detect biotinylated antibodies. Dead cells were excluded by positivity for 7-aminoactinomycin D (7-AAD) (Invitrogen). Flow cytometric acquisition was performed on a BD LSR II flow cytometer (BD Biosciences), and cell sorting was performed on a BD FACSAria II flow cytometer (BD Biosciences). Data were analyzed using FlowJo software (TreeStar).

Peptides and MHC tetramers. The following class I-restricted peptides were used: M45$_{985–993}$, m139$_{419–426}$, M38$_{316–323}$, IE3$_{416–423}$, M57$_{816–824}$, M33$_{47–55}$, M44$_{130–138}$, M78$_{8–15}$, M86$_{1062–1070}$, and m141$_{16–23}$. The following class II-restricted peptides were used: m09$_{133–147}$, M25$_{409–423}$, m139$_{560–574}$, and m142$_{24–38}$. MHC class I tetramers for MCMV M45 (D^b restricted), M57, m139, M38, and IE3 (all K^b restricted) and for LCMV GP$_{33}$ and NP$_{396}$ (both D^b restricted) were produced as described elsewhere (30).

Adoptive transfers, *in vivo* cell division, and secondary expansion. Splenic CD8$^+$ T cells were used for adoptive transfer experiments and were isolated using a CD8$^+$ T cell enrichment kit (Miltenyi Biotec) according to the manufacturer's protocol. Naive Thy1.1 (or Ly5.2) recipients received 8×10^6 CD27$^{+/+}$ (Ly5.1 and Thy1.2) CD8$^+$ T cells and 8×10^6 CD27$^{-/-}$ (Ly5.2 and Thy1.2) CD8$^+$ T cells via retro-orbital injection, and 24 h later these mice were infected with 1×10^4 PFU MCMV-Smith. One week prior to the CD8$^+$ T cell adoptive transfer, Thy1.1 mice received 75 μg of a CD8$^+$ T cell-depleting antibody (clone 2.43) via i.p. injection to facilitate the expansion of the newly introduced CD8$^+$ T cells. At the time of adoptive transfer, ~1% host CD8$^+$ T cells were detected in the blood. On day 8 postinfection, the magnitude and phenotype of the MCMV-specific CD8$^+$ T cell response (specifically of the adoptively transferred CD27$^{+/+}$ Ly5.1 and CD27$^{-/-}$ Ly5.2 CD8$^+$ T cells) were determined by tetramer staining combined with staining for congenic markers (Ly5.1, Ly5.2, Thy1.1, and Thy1.2) and CD127.

To determine *in vivo* cell division, 5×10^6 CD8$^+$ T cells isolated from naive WT or CD27$^{-/-}$ mice were labeled with 2.5 μM carboxyfluorescein succinimidyl ester (CFSE; Invitrogen) and adoptively transferred into naive Ly5.1 mice that were depleted of CD8$^+$ T cells as described above. All mice were infected with 1×10^4 PFU MCMV-Smith 3 h later. At day 3 postinfection, cell division was determined by analyzing the CFSE dilution profiles of the adoptively transferred CD8$^+$ T cells in the spleen.

To determine the secondary expansion capacity of memory CD8$^+$ T cells that developed during proficient or deficient CD27 costimulation, i.e., WT and CD27$^{-/-}$ memory CD8$^+$ T cells, mice were infected with 1×10^4 PFU MCMV-Δm157. At day 45 postinfection, M45- and M38-specific CD8$^+$ T cells were sorted, and 2×10^3 M45- and 5×10^3 M38-specific WT or CD27$^{-/-}$ CD8$^+$ T cells were transferred via retro-orbital injection into naive Thy1.1 mice. Smaller numbers of M45-specific CD8$^+$ T cells than M38-specific T cells were transferred, as this reflects the *in vivo* situation in case of reinfection. The recipient mice were infected 3 h later with 1×10^4 PFU MCMV-Smith or MCMV-Δm157, and at day 7 postinfection, the fold expansion of the donor M45- and M38-specific CD8$^+$ T cell populations in the spleen was determined by tetramer staining. The absolute numbers of donor M45- or M38-specific Thy1.2$^+$ CD8$^+$ T cells in the spleen were determined by multiplying the frequencies of these cells in the total splenic population by the total number of splenic cells. Fold expansion was calculated by dividing the absolute numbers of donor M45- and M38-specific CD8$^+$ T cells in the spleen by the number of adoptively transferred cells. To determine the secondary expansion of CD27-proficient (WT) memory CD8$^+$ T cells in a situation where CD27-CD70 costimulation is lacking during rechallenge, Thy1.1 mice were infected with MCMV-Smith. At day 45 postinfection, M38-specific CD8$^+$ T cells were sorted, and 4×10^3 M38-specific CD8$^+$ T cells were transferred i.v. into Thy1.2 recipients that received blocking anti-CD70 or control IgG before and after transfer (at days -1, 0, and 3). Recipient mice were infected with 1×10^4 PFU MCMV-Smith 3 h after adoptive transfer. Fold expansion was calculated at day 7 postinfection, by dividing the absolute number of Thy1.1$^+$ M38-specific CD8$^+$ T cells in the spleen by the number of adoptively transferred M38-specific CD8$^+$ cells.

To determine the expansion, survival, and secondary expansion capacity of WT OT-I and CD27$^{-/-}$ OT-I cells, 2×10^3 cells were transferred via retro-orbital injection into naive Ly5.1 recipients. Recipient mice were infected 3 h later with 5×10^5 PFU MCMV-OVA. At day 7 and later time points postinfection, the percentage of OT-I T cells in the blood was determined. Six months after primary infection, recipients received a secondary infection with 5×10^5 PFU MCMV-OVA, and 5 days later, the percentage of OT-I T cells in the spleen was determined.

In vivo cytotoxicity assay. Splenocytes of naive Ly5.1 mice were loaded with class I peptides (M45, M38, and IE3) for 1 h at 37°C or were used unpulsed (no-peptide control). After extensive washing, cells were labeled with high or low concentrations of CFSE (Invitrogen) and the proliferation dye eFluor670 (eBioscience). Populations were pooled and injected i.v. (5×10^6 per labeled population) into naive mice or CD27$^{-/-}$ or WT mice that had been infected 8 or 30 days before with 1×10^4 PFU MCMV-Δm157. After 3 h (day 8 postinfection) or 5 h (day 30 postinfection), spleens were isolated from recipient mice, and killing was determined by flow cytometry. The relative survival of each population was calculated compared to the same population in naive recipients by using the following formula: {100 − [(percentage of pulsed peptide in infected mice/percentage of unpulsed peptide in infected mice)/(percentage of pulsed peptide in naive mice/percentage of unpulsed peptide in naive mice)]} × 100.

Statistical analysis. Statistical significance of the cellular responses was determined with the Student *t* test. Statistical significance of viral titers was determined with the Mann-Whitney test. P values of <0.05 were considered significant. GraphPad Prism software was used for all statistical analyses.

RESULTS

Loss of CD27 expression uniquely identifies inflationary memory T cells during CMV infection. In humans, a strong correlation has been found between HCMV seropositivity and the loss of CD27 expression on HCMV-specific T cells (17–20). To determine the kinetics of CD27 expression on MCMV-specific T cells, mice were infected with MCMV-Smith, and noninflationary (M45-specific) and inflationary (m139-, M38-, and IE3-specific)

CD8$^+$ memory T cell responses (14) were longitudinally followed in the blood by combined tetramer and CD27 staining (Fig. 1A and B). During acute MCMV infection, both noninflationary and inflationary T cell populations expressed high levels of CD27, whereas in persistent CMV infection, specifically the inflationary T cells gradually lost the expression of CD27. This loss of CD27 expression on MCMV-specific inflationary T cells, however, does not reflect an absolute downregulation (see comparison with CD27$^{-/-}$ CD8$^+$ T cells in Fig. 1F).

To determine if the loss of CD27 on virus-specific T cells is a general phenomenon observed during persistent infections, mice were infected with two different strains of LCMV that establish either a chronic (clone 13) or acute (Armstrong) infection (31). In contrast to MCMV-specific inflationary T cells, the majority of the LCMV-specific CD8$^+$ T cells retained CD27 expression throughout both acute and chronic infections (Fig. 1C and D). The expression levels of CD27 on noninflationary MCMV- and LCMV-specific T cells were comparable (Fig. 1E). Taken together, these data indicate that the loss of CD27 appears to be specific for inflationary memory CD8$^+$ T cells during persistent CMV infection.

CMV-specific CD4$^+$ T cell responses are dependent on CD70-mediated costimulation. To determine the physiological role of CD27-CD70 interactions in CMV infection, CD70-mediated costimulation was inhibited during acute MCMV infection by the administration of a blocking, nondepleting anti-CD70 antibody (clone FR70) (32). At early time points postinfection, no differences in viral load were observed in the livers and lungs of control antibody-treated mice and mice with CD70 blockade (Fig. 2A). The absolute number of NK1.1$^+$ CD3$^-$ cells in the spleen was also not significantly different at day 3 following infection, which is consistent with a comparable viral load (Fig. 2B). Furthermore, a similar expression of the early activation marker CD69 was found on NK1.1$^+$ CD3$^-$ cells at this time (Fig. 2C). These results indicate that CD27-CD70 interactions do not substantially alter the NK cell activity and viral load during the very early phases of acute CMV infection.

At day 8 postinfection, however, the viral load in the salivary glands was higher in mice with abrogated CD27-CD70 interactions (Fig. 2D). To examine whether CD4$^+$ or CD8$^+$ T cells control viral replication at this time point after infection, these T cell subsets were depleted upon infection. Whereas in the absence of CD4$^+$ T cells the viral titer was increased in the salivary glands, depletion of CD8$^+$ T cells had no effect on viral control (Fig. 2E). Also, at day 30 postinfection, anti-CD70 antibody-treated mice had increased virus production in the salivary glands compared to control antibody-treated mice (Fig. 2D). At this time point, CD4$^+$ T cells still play a critical role in controlling CMV replication in tissues, especially in the salivary glands (10, 28, 33). To determine the importance of CD27-CD70 interactions for the development of MCMV-specific CD4$^+$ T cell responses, we determined the magnitude of this response in anti-CD70 and control antibody-treated mice by intracellular cytokine staining after restimulation with MCMV-specific class II-restricted peptides (16). The CD4$^+$ T cell responses to various class II epitopes were reduced ~2-fold in mice with abrogated CD27-CD70 interactions (Fig. 2F), indicating that CD27-CD70 costimulation regulates viral replication via downsizing CMV-specific CD4$^+$ T cell responses.

CD27-CD70 costimulation promotes the expansion of CMV-specific CD8$^+$ T cells during acute CMV infection. To determine the role of CD27-CD70 costimulation in regulating the
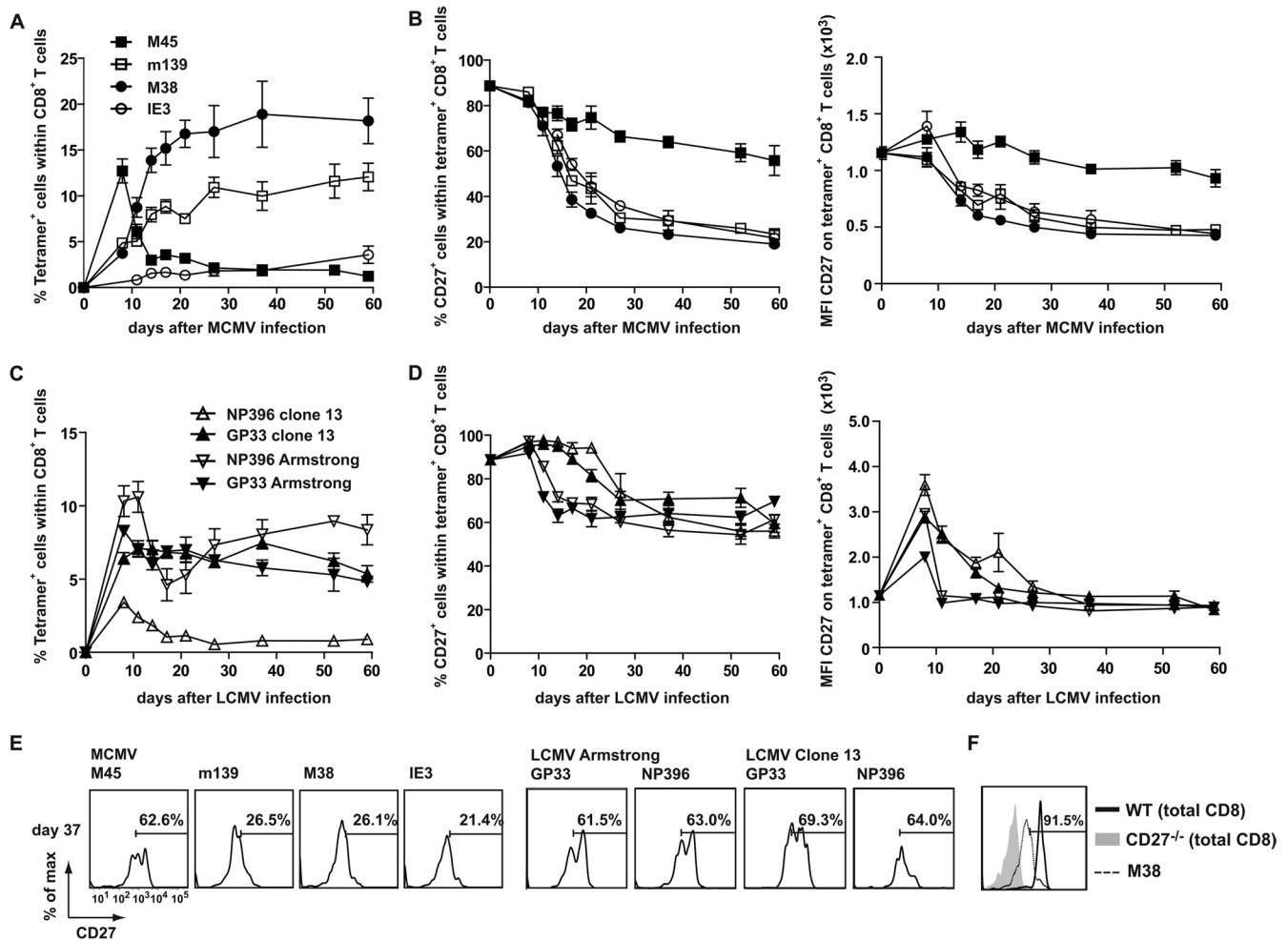
FIG 1 Loss of CD27 expression uniquely identifies inflationary memory CD8$^+$ T cells. (A) WT mice were infected with 5×10^4 PFU MCMV-Smith, and at the indicated times, the CD8$^+$ T cell responses to epitopes derived from MCMV proteins (M45, m139, M38, and IE3) were examined in blood. The graph shows the frequency of MCMV-specific CD8$^+$ T cells for each epitope, identified using MHC class I tetramers. (B) Cell surface expression of CD27 on MCMV-specific CD8$^+$ T cells. The graphs show the percentages of tetramer$^+$ CD8$^+$ T cells expressing CD27 and the mean fluorescence intensities (MFI) for CD27 of tetramer$^+$ CD8$^+$ T cells. (C) Mice were infected with LCMV Armstrong or LCMV clone 13, and at the indicated times, the percentages of GP$_{33}$- and NP$_{396}$-specific CD8$^+$ T cells in blood were determined by MHC class I tetramer staining. (D) Cell surface expression of CD27 on LCMV-specific CD8$^+$ T cells. The graphs show the percentages of tetramer$^+$ CD8$^+$ T cells expressing CD27 and the MFI for CD27 of tetramer$^+$ CD8$^+$ T cells. (E) Representative histograms showing cell surface expression of CD27 on tetramer$^+$ CD8$^+$ T cells 37 days after infection with MCMV-Smith, LCMV Armstrong, or LCMV clone 13. (F) Histogram showing expression of CD27 on total CD8$^+$ T cells of naive WT or CD27$^{-/-}$ mice. CD27 expression on M38$^+$ CD8$^+$ T cells 37 days after infection with MCMV-Smith is also shown. All experiments were performed twice with similar results. Data shown are mean values and standard errors of the means (SEM) ($n = 4$).

magnitude of CMV-specific CD8$^+$ T cell responses, both noninflationary (stable) and inflationary responses were analyzed by MHC class I tetramer staining. On day 8 following infection, the response to the noninflationary epitope M45 was reduced ∼3-fold in mice with abrogated CD27-CD70 costimulation compared to control mice (Fig. 3A and B). In addition, the magnitude of the m139-specific CD8$^+$ T cell response, which expands similarly to M45-specific responses during acute MCMV infection but has inflationary properties during the persistent phase of infection, was reduced ∼2.5-fold. No significant differences were observed for the M38-specific CD8$^+$ T cell response, indicating that this inflationary epitope is less dependent on CD27-CD70 costimulation in the acute phase of MCMV infection.

Recently, it was found that during certain influenza virus infections CD27-deficient mice had an increased binding of te-

tramer on antigen-specific CD8$^+$ T cells on a per-cell basis than WT mice, suggesting that CD27 promotes T cell responses with low affinity (34). In this study, however, no differences in tetramer binding were found on a per-cell basis on MCMV-specific CD8$^+$ T cells between mice with abrogated CD27-CD70 interaction and control mice (Fig. 3A).

To confirm the findings obtained with anti-CD70 blocking antibodies, WT and CD27 gene-targeted knockout (CD27$^{-/-}$) mice (22) were infected with MCMV-Smith. Unexpectedly, several days after infection, all knockout animals suffered from CMV disease, which was reminiscent of an NK cell defect, as these cells limit early acute infection. The Ly49 gene cluster is in close proximity to the targeted CD27 gene (∼2 centimorgans [cM]), and therefore we focused specifically on analyzing the Ly49H gene product, since Ly49H (i) is deficient in the original mouse strain
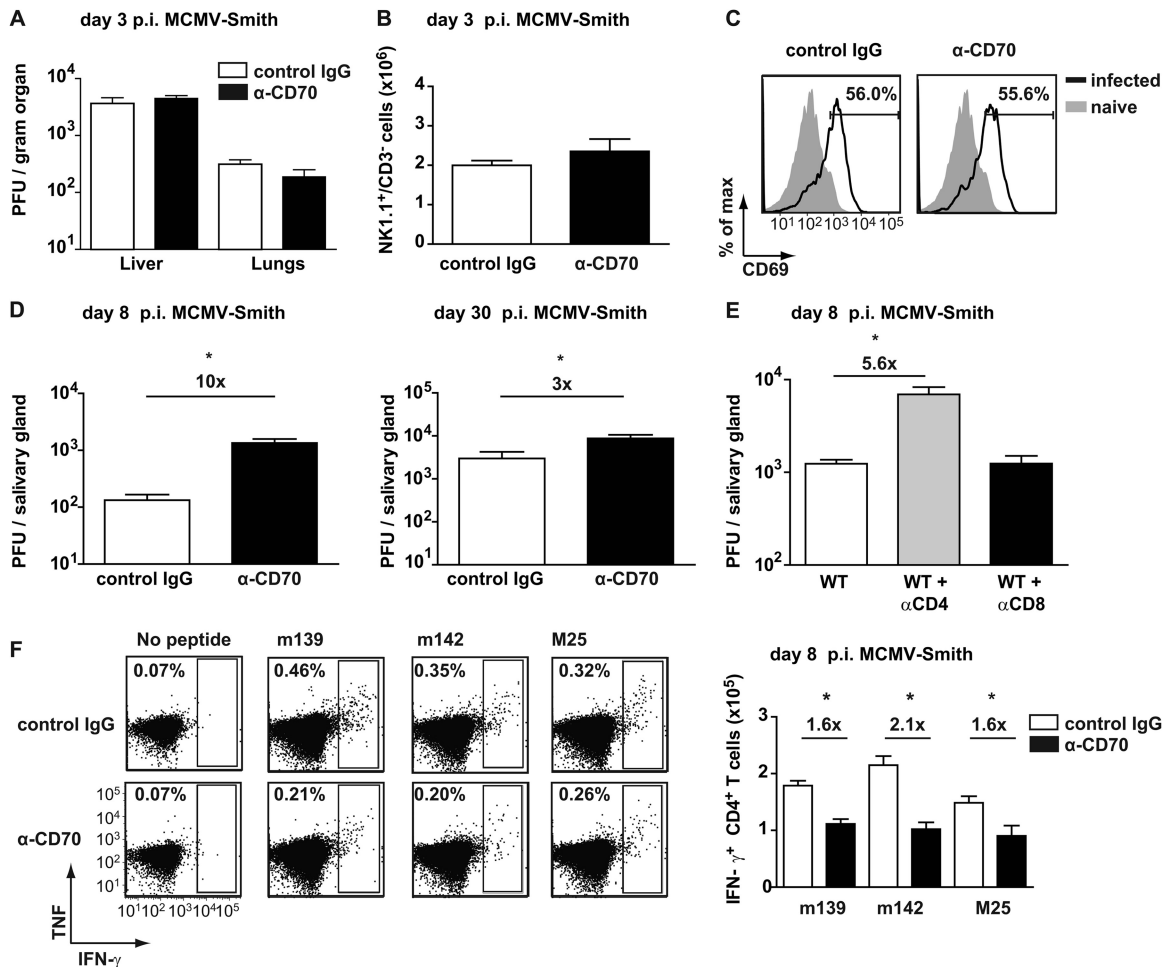
FIG 2 Viral control and MCMV-specific CD4$^+$ T cell expansion are dependent on CD27-CD70 costimulation. (A) WT mice infected with 1×10^4 PFU MCMV-Smith were treated with blocking anti-CD70 (α-CD70) or control antibody. The graph shows the viral titers in the liver and lungs, determined by plaque assays at day 3 postinfection (p.i.). (B) The absolute numbers of NK1.1$^+$CD3$^-$ cells in the spleen were determined at day 3 postinfection. The graph shows means and SEM ($n = 5$ mice per group). (C) Representative plots showing expression of CD69 on NK1.1$^+$CD3$^-$ cells from naive (gray filled histograms) and infected (solid black lines) mice. Numbers indicate the percentages of NK1.1$^+$CD3$^-$ cells positively stained for CD69. (D) At day 8 and day 30 postinfection, the viral titers in the salivary glands were determined by plaque assays. (E) WT mice were infected with 5×10^4 PFU MCMV-Smith and were depleted of CD4$^+$ and CD8$^+$ T cells by use of antibodies. The graph shows the viral titers in the salivary glands at day 8 postinfection. (F) WT mice infected with 1×10^4 PFU MCMV-Smith were treated with blocking anti-CD70 (α-CD70) or control antibody, and at day 8 postinfection, the MCMV-specific CD4$^+$ T cell responses to m139, m142, and M25 in the spleen were determined by intracellular cytokine staining. Representative flow cytometry plots show the frequencies of splenic CD4$^+$ T cells producing IFN-γ and TNF. The bar graph shows the absolute numbers of IFN-γ-producing CD4$^+$ T cells (means + SEM). Fold differences are indicated. Experiments were performed twice with similar results. For all experiments, the statistical significance of differences in viral titers was determined with the Mann-Whitney test, and that for cellular responses was determined with the Student t test (*, $P < 0.05$; $n = 4$ or 5 mice per group).

(129/Ola) that was used to generate the CD27$^{-/-}$ mice; and (ii) is known to be important for NK cell activation during MCMV infection in Ly49H$^+$ mice (such as C57BL/6 strains), due to its interaction with the MCMV protein m157 (35). Although naive CD27$^{-/-}$ mice contained normal absolute numbers of NK cells, the NK cell receptor Ly49H was absent (Fig. 3C). Likely due to the low chance of separation of the CD27 gene and the Ly49 gene cluster, the Ly49H gene is missing in CD27$^{-/-}$ mice backcrossed on a C57BL/6 background, which is consistent with a recent report that showed that CD27$^{-/-}$ NK cells exhibit a 129/P2Ola-founded NK cell repertoire (36). To overcome this defect of Ly49H-dependent NK cell activation in CD27$^{-/-}$ mice upon MCMV infection, an MCMV mutant lacking m157 (i.e., MCMV-Δm157) was used. MCMV-Δm157 was generated on the MCMV BAC pSM3fr (37)

and is less virulent than the salivary gland-derived strain MCMV-Smith. In line with the data obtained with the CD70 blockade, at day 8 following infection the virus-specific CD8$^+$ T cell expansion in the spleens, livers, and lungs of MCMV-Δm157-infected CD27$^{-/-}$ mice was reduced compared to that in infected WT mice (Fig. 3D). Significantly decreased numbers of MCMV-specific CD4$^+$ T cells were also observed in CD27$^{-/-}$ mice (data not shown).

To determine if CD27-CD70 interactions are broadly important for the expansion of CMV-specific T cells, additional responses were analyzed by intracellular IFN-γ staining after peptide restimulation. Initially, we verified that the percentages of IFN-γ-producing CD8$^+$ T cells correlated with the percentages of class I tetramer$^+$ cells (Fig. 3E and F). As expected, the magnitudes
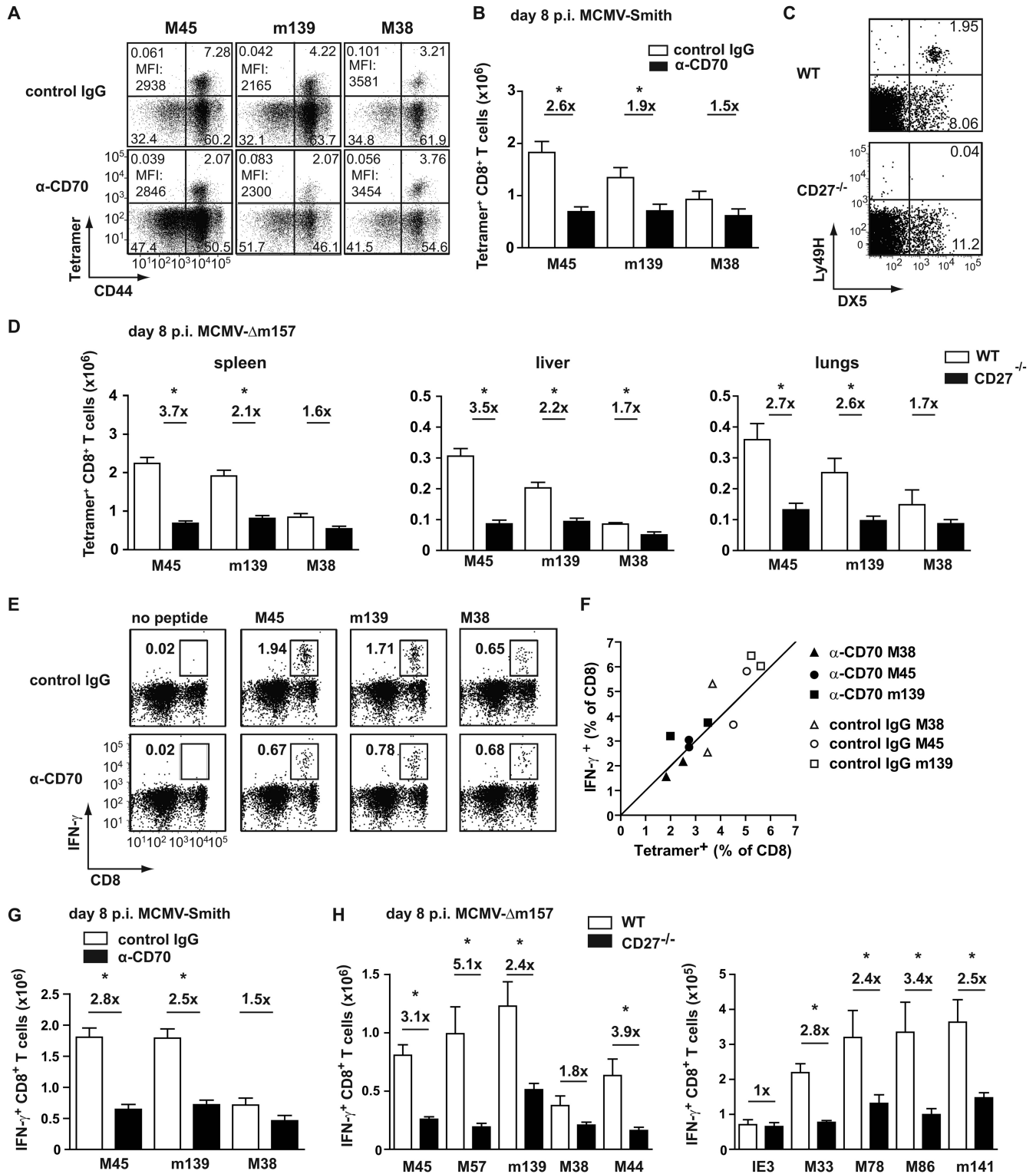
FIG 3 CD27-CD70 costimulation controls the magnitude of MCMV-specific CD8^{+} T cells in acute infection. (A) Mice were infected with 1×10^4 PFU MCMV-Smith, and a blocking anti-CD70 or control antibody was administered. At day 8 postinfection, splenic CD8^{+} T cells were assessed for CD44 expression and binding to MHC class I tetramers. Data shown are representative flow cytometry plots gated on CD8^{+} T cells. Percentages in each quadrant and average MFI of tetramer^{+} CD44^{+} cells are indicated. (B) Total numbers of splenic MCMV-specific CD8^{+} T cells. Pooled data from two independent experiments are shown. (C) Representative flow cytometry plots showing cell surface staining of DX5 and Ly49H on splenocytes of naive wild-type and naive CD27^{−/−} mice. (D) WT and CD27^{−/−} mice were infected with 1×10^4 PFU MCMV-Δm157, and at the indicated times, the MCMV-specific CD8^{+} T cell responses were determined by MHC class I tetramer staining. Graphs depict the total numbers of MCMV-specific CD8^{+} T cells in the spleen, liver, and lungs on day 8 postinfection. Pooled data from two independent experiments are shown. (E) WT mice were infected with 1×10^4 PFU MCMV-Smith, and a CD70-blocking or control antibody was
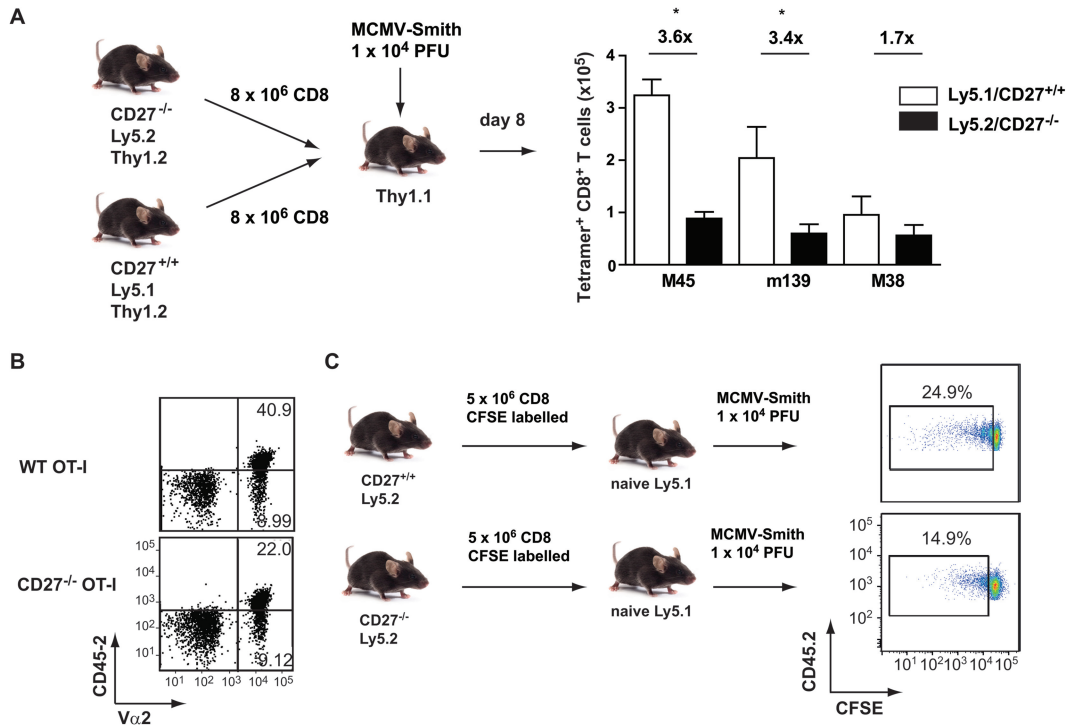
FIG 4 CD27 costimulation directly influences the expansion of MCMV-specific CD8$^+$ T cells. (A) Schematic of adoptive transfer experiment. CD8$^+$ T cells were isolated from CD27$^{-/-}$ Ly5.2$^+$ and CD27$^{+/+}$ Ly5.1$^+$ mice and subsequently transferred in a 1:1 ratio into naive Thy1.1 congenic hosts. Recipients were subsequently infected with 1 × 10^4 PFU MCMV-Smith, and 8 days later, the MCMV-specific CD8$^+$ T cell responses in the spleen were determined by MHC class I tetramer staining. The graph depicts total numbers of CD27$^{-/-}$ Ly5.2$^+$ and CD27$^{+/+}$ Ly5.1$^+$ T cells. Fold differences are indicated. Experiments were performed twice with similar results. (B) A total of 2 × 10^3 CD45.2$^+$ naive CD27$^{-/-}$ or wild-type TCR transgenic OT-I cells were isolated and transferred into naive Ly5.1 recipients, which were subsequently infected with 5 × 10^5 PFU MCMV-OVA. Cell surface staining was performed on the blood at 7 days postinfection. Representative flow cytometry plots show percentages of Ly5.2 and Vα2 within CD8$^+$ T cells. (C) Schematic of adoptive transfer experiment. CD8$^+$ T cells were isolated from naive CD27$^{-/-}$ and WT mice, labeled with CFSE, and transferred into naive Ly5.1 mice, which were subsequently infected with 1 × 10^4 PFU MCMV-Smith. Representative flow cytometry plots show CFSE dilution of CD45.2$^+$ T cells at day 3 postinfection. Cells were gated on CD45.2$^+$ and CD8$^+$ ($n = 4$).

of the M45- and m139-specific CD8$^+$ T cell responses as determined by IFN-γ production were reduced 2- to 3-fold in mice with abrogated CD27-CD70 interactions (Fig. 3G and H). CMV-specific CD8$^+$ T cell responses against a number of noninflationary epitopes (M57, M44, M33, M78, M86, and m141) were all reduced in CD27$^{-/-}$ mice. However, the magnitude of the inflationary IE3 response was not affected by CD70 blockade at day 8 postinfection. Together, these results show that CD27-CD70 costimulation in acute MCMV infection is important predominantly for the expansion of MCMV-specific CD8$^+$ T cells that establish stable memory T cell pools.

CD27-CD70 costimulation has a direct effect on the expansion of MCMV-specific CD8$^+$ T cells. To examine if the reduced expansion of the MCMV-specific CD8$^+$ T cell response in mice with abrogated CD27-CD70 interaction was caused by direct effects through CD27 expression on CD8$^+$ T cells or due to another mechanism (e.g., CD27 expression on other immune cells or ex-

posure to different viral titers), adoptive T cell transfers of congenically marked CD27-proficient (CD27$^{+/+}$ Ly5.1) CD8$^+$ T cells and CD27-deficient (CD27$^{-/-}$ Ly5.2) CD8$^+$ T cells were performed with the same host mice (Thy1.1), which were subsequently infected with MCMV-Smith (Fig. 4A). At day 8 postinfection, the M45- and m139-specific responses in the spleen were reduced ~3.5-fold for CD27$^{-/-}$ CD8$^+$ T cells in comparison with WT CD8$^+$ T cells, indicating a direct role for CD8$^+$ T cell-expressed CD27. Similar results were observed when the recipient mice were infected with MCMV-Δm157 (data not shown), which excludes possible effects of T cell-expressed Ly49H. In addition, when naive CD27$^{-/-}$ and WT TCR transgenic OT-I cells were adoptively transferred into naive congenic Ly5.1 host mice, the percentage of WT OT-I cells observed in the blood at day 7 after infection with MCMV-OVA was twice as high as the percentage of CD27$^{-/-}$ OT-I cells (Fig. 4B).

To test the impact of CD27-CD70 costimulation on T cell di-

administered. At day 8 postinfection, the MCMV-specific CD8$^+$ T cell responses in the spleen were analyzed by intracellular cytokine staining upon peptide restimulation. Data shown are representative flow cytometry plots of CD8$^+$ T cells producing IFN-γ. Percentages are for CD8$^+$ IFN-γ$^+$ T cells within the live gate. (F) Percentages of tetramer$^+$ CD8$^+$ T cells versus IFN-γ-producing CD8$^+$ T cells. (G) Total numbers of IFN-γ$^+$ CD8$^+$ T cells per spleen. Fold differences are indicated. Pooled data from two independent experiments are shown. (H) WT and CD27$^{-/-}$ mice were infected with 1 × 10^4 PFU MCMV-Δm157. At day 8 postinfection, the MCMV-specific CD8$^+$ T cell responses in the spleen were determined by intracellular cytokine staining upon restimulation with the indicated class I peptides. Fold differences are indicated. All bar graphs show means and SEM. Statistical significance was determined with the Student t test (*, $P < 0.05$; $n = 4$ to 8).
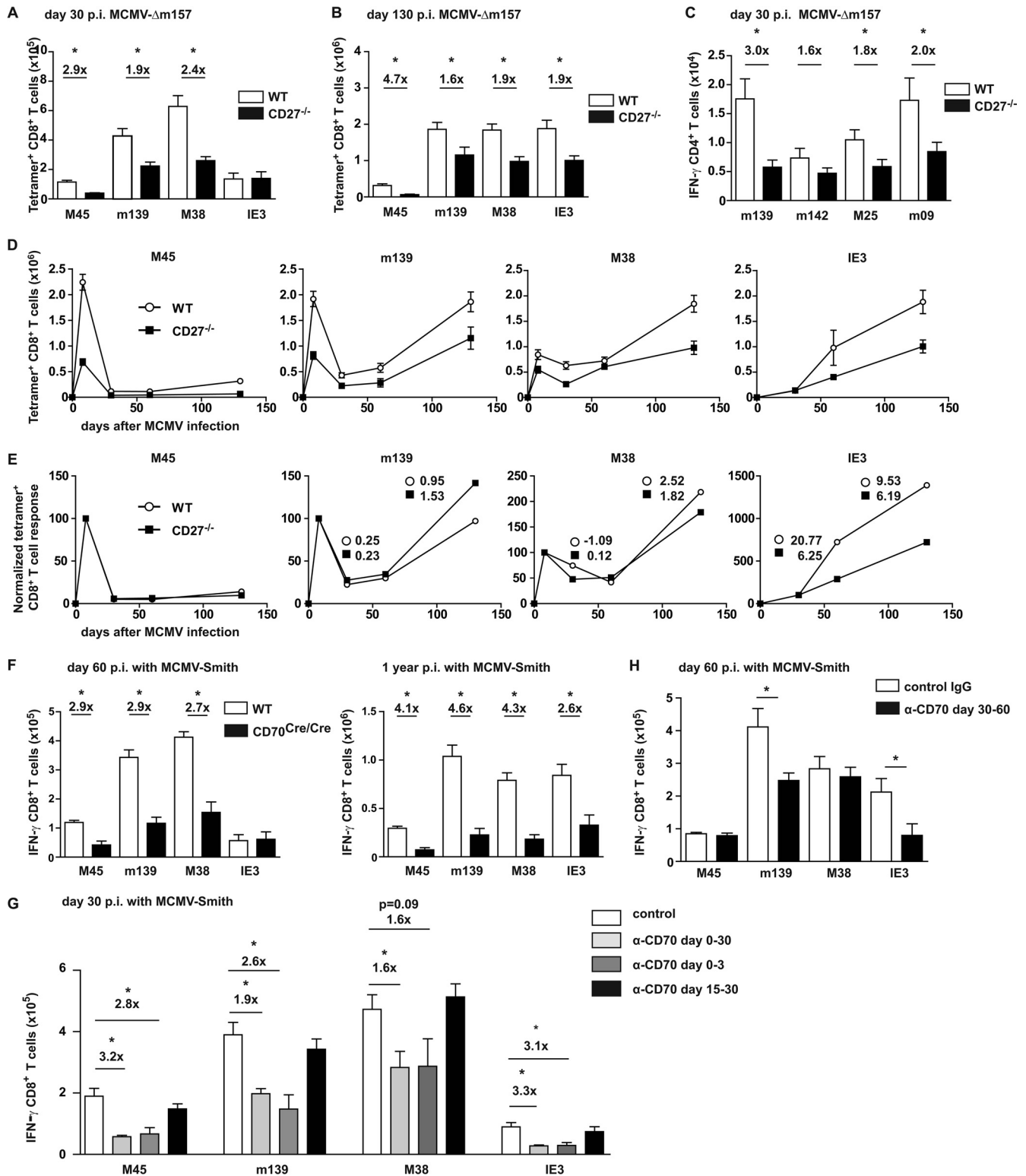
FIG 5 CD27-CD70 interactions are important for the accumulation of inflationary memory CD8$^+$ T cells. (A and B) WT and CD27$^{-/-}$ mice were infected with 1×10^4 PFU MCMV-Δm157. At day 30 (A) and day 130 (B) postinfection, the MCMV-specific CD8$^+$ T cell responses in the spleen were determined by MHC class I tetramer staining. (C) At day 30 postinfection, the MCMV-specific CD4$^+$ T cell responses in the spleen were determined by intracellular cytokine staining after restimulation with indicated class II-restricted peptides. (D) Kinetics of absolute numbers of MCMV-specific CD8$^+$ T cells in the spleen. (E) Kinetics of normalized MCMV-specific CD8$^+$ T cell responses. MCMV-specific CD8$^+$ T cell responses in the spleen were normalized to the peak of the response at 8 days postinfection, except for the IE3-specific response, which was normalized to the response on day 30 postinfection. The slopes of normalized expression curves between days 30 to 60 and days 60 to 130 are indicated for inflationary responses. (F) WT and CD70$^{Cre/Cre}$ mice were infected with 1×10^4 and 5×10^4 PFU MCMV-Smith at 60 days and 1 year postinfection, respectively, and the MCMV-specific CD8$^+$ T cell responses in the spleen were determined by intracellular

vision, naive CFSE-labeled CD8$^+$ T cells of WT and CD27$^{-/-}$ mice were transferred into naive congenic Ly5.1 mice, which were subsequently infected with MCMV-Smith. Three days later, the percentage of divided CD27$^{-/-}$ CD8$^+$ T cells was lower (average, 14.9% ± 0.81%) than that of WT CD8$^+$ T cells (average, 26.9% ± 2.47%) (Fig. 4C), indicating a direct impact of CD27 signals on T cell division. Together, these data show that CD27 costimulation acts directly on MCMV-specific CD8$^+$ T cells and promotes the expansion of these cells during acute infection.

CD27-CD70 costimulation contributes to the inflation of CMV-specific memory T cells. In persistent MCMV infection, the T cell pool is dominated by cells that undergo memory T cell inflation (15). To examine if CD27-CD70 interactions are critical for the accumulation of inflationary memory T cells, T cell responses in wild-type and CD27$^{-/-}$ mice infected with MCMV-Δm157 were analyzed longitudinally. As observed in acute infection, M45- and m139-specific CD8$^+$ T cell responses in the spleen were reduced in CD27$^{-/-}$ mice at day 30 postinfection (Fig. 5A). Strikingly, the magnitude of the M38-specific CD8$^+$ T cell response was also significantly lower in mice with abrogated CD27-CD70 interactions. Moreover, the inflation of splenic IE3-specific CD8$^+$ T cells between day 30 and day 130 was diminished in CD27$^{-/-}$ mice (Fig. 5A, B, and D). Normalization of the kinetics of MCMV-specific CD8$^+$ T cell responses confirmed that M38- and IE3-specific CD8$^+$ T cell responses have a diminished inflation pattern in chronic infection (Fig. 5E). Similar to what was found at day 8 following infection, MCMV-specific CD4$^+$ T cell responses were significantly reduced in CD27$^{-/-}$ mice during the persistent phase, including the inflationary response against the m09 epitope (Fig. 5C).

To corroborate the findings on the development of T cell responses during persistent infection obtained with CD27$^{-/-}$ mice infected with MCMV-Δm157, we performed additional experiments with CD70$^{Cre/Cre}$ mice (23) infected with MCMV-Smith. On day 60 following infection, the magnitudes of the noninflationary M45- and inflationary M38- and m139-specific CD8$^+$ T cell responses were significantly decreased in CD70$^{Cre/Cre}$ mice compared to wild-type mice (Fig. 5F). At later time points (>100 days postinfection), the accumulation of inflationary IE3-specific T cells was also affected by the lack of CD27-CD70 costimulation (Fig. 5F). Overall, these data show that CD27-CD70 costimulation contributes to the development of both stable and inflationary T cell responses during persistent CMV infection.

To examine the timing of importance of CD27-CD70 costimulation relative to the development of CMV-specific T cell pools, interactions between CD27 and CD70 were blocked with anti-CD70 antibodies at several time points postinfection, and the magnitudes of the MCMV-specific T cell responses were determined. Both acute and inflationary MCMV-specific T cell responses were severely reduced when CD27-CD70 interactions were either continuously abrogated or blocked in the beginning of infection. However, blocking of CD27-CD70 signals from day 15

to day 30 did not significantly alter the magnitudes of the MCMV-specific CD8$^+$ T cell responses (Fig. 5G), indicating that CD27-CD70 costimulation during this time postinfection has no critical role. Blocking CD27-CD70 interactions from day 30 to day 60 following infection obstructed the inflationary CD8$^+$ T cell responses specific for m139 and IE3 (Fig. 5H).

Long-term administration of allogeneic IgG, such as rat IgG, in mice can result in rapidly cleared immune complexes and consequent loss of efficacy. To test whether FR70 (rat anti-mouse CD70) could still be detected in the sera of mice that received long-term treatment with this antibody, a rat IgG-specific ELISA was performed. In all infected mice that received anti-CD70 antibody, levels of rat IgG of up to 600 ng/ml were detected in the serum (data not shown), indicating the presence of circulating FR70 despite long-term administration. In infected mice that did not receive antibody, rat IgG was not measurable. In conclusion, CD27-CD70 costimulation influences the magnitude of the MCMV-specific CD8$^+$ T cell pool mainly in the beginning of infection and is also moderately implicated in the accumulation of inflationary MCMV-specific CD8$^+$ T cells during persistent MCMV infection.

The downmodulation of CD27 on MCMV-specific CD8$^+$ T cells is ligand independent. The expression of CD27 can be downregulated by interaction with its ligand CD70 and upon repeated antigenic stimulation (38–40). To determine if the loss of CD27 expression observed for inflationary T cells in chronic MCMV infection is mediated by CD70, combined tetramer and CD27 staining was performed for mice in which CD27-CD70 interaction was abrogated with a blocking anti-CD70 antibody. At day 30 postinfection, in anti-CD70 and control antibody-treated mice, the inflationary M38-specific CD8$^+$ T cells that were present in blood, but also in the spleen and lungs, had a loss of CD27 expression, while the noninflationary M45-specific CD8$^+$ T cells expressed high levels of CD27 (Fig. 6A). Importantly, anti-CD70 and control antibody-treated mice had similar levels of CD27 on these MCMV-specific CD8$^+$ T cell populations (Fig. 6A), and these results were recapitulated in CD70$^{Cre/Cre}$ mice (Fig. 6B), suggesting that the loss of CD27 expression during CMV infection is not mediated by interaction with CD70 but by persistent antigenic stimulation.

Effects of CD27-CD70 costimulation on cell surface molecules of CMV-specific CD8$^+$ T cells. To examine whether CD27-CD70 costimulation influences the differentiation and activation condition of MCMV-specific T cells, the expression of cell surface molecules on MHC class I tetramer-binding CD8$^+$ T cells was analyzed. A significant reduction in the expression of CD127 (IL-7 receptor alpha [IL-7Rα]) was found at day 8 postinfection, on both stable and inflationary T cells (Fig. 7A and B), for mice treated with anti-CD70 antibody compared to control antibody-treated mice. Cell surface molecules involved in T cell migration (CD44, CD62L, and CXCR3), activation (KLRG1), costimulation (CD27 and PD-1), and IL-2 signaling (CD25) were not differen-

IFN-γ$^+$ staining. (G) Mice were infected with 1×10^4 PFU MCMV-Smith and received the blocking anti-CD70 antibody from days −1 to 30, days −1 to 3, or days 15 to 30 following infection. At day 30 postinfection, the MCMV-specific CD8$^+$ T cell responses in the spleen were determined by intracellular IFN-γ$^+$ staining. Pooled data from three independent experiments are shown as means + SEM. (H) Mice were infected with 1×10^4 PFU MCMV-Smith and received a blocking anti-CD70 or control antibody from day 30 to day 60 following infection. At day 60 postinfection, the MCMV-specific CD8$^+$ T cell responses in the spleen were determined by intracellular cytokine staining. All bar graphs show means + SEM, and fold differences are indicated. Statistical significance was determined with the Student t test (*, $P < 0.05$; n = 5 to 12).
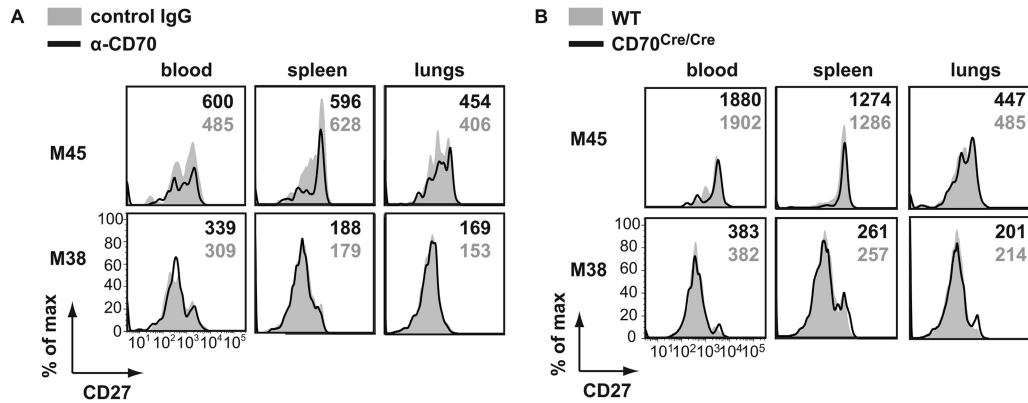
FIG 6 Downmodulation of CD27 on MCMV-specific CD8$^+$ T cells is not dependent on interaction with CD70. (A and B) The expression of CD27 on splenic MHC class I-binding CD8$^+$ T cells during chronic MCMV infection was determined by cell surface staining of cells from mice that received a blocking anti-CD70 antibody (solid black lines) or a control antibody (filled gray histograms) from days 0 to 30 postinfection (A) and for CD70$^{Cre/Cre}$ (solid black lines) and wild-type (filled gray histograms) mice (B). The MFI of CD27 expression on tetramer$^+$ CD8$^+$ T cells are indicated. Representative histograms for one of five mice are shown.

tially expressed (Fig. 7A). Also, in MCMV-Δm157-infected CD27$^{-/-}$ mice, the expression levels of CD127 but not other cell surface molecules were decreased (data not shown). During chronic infection, no differences in the expression of CD127 (as well as other markers, including CD44, CD62L, and KLRG1) were found between WT and CD27$^{-/-}$ mice (data not shown).

To examine whether the decreased CD127 expression at early time points postinfection was due to a direct effect of CD27 trig-
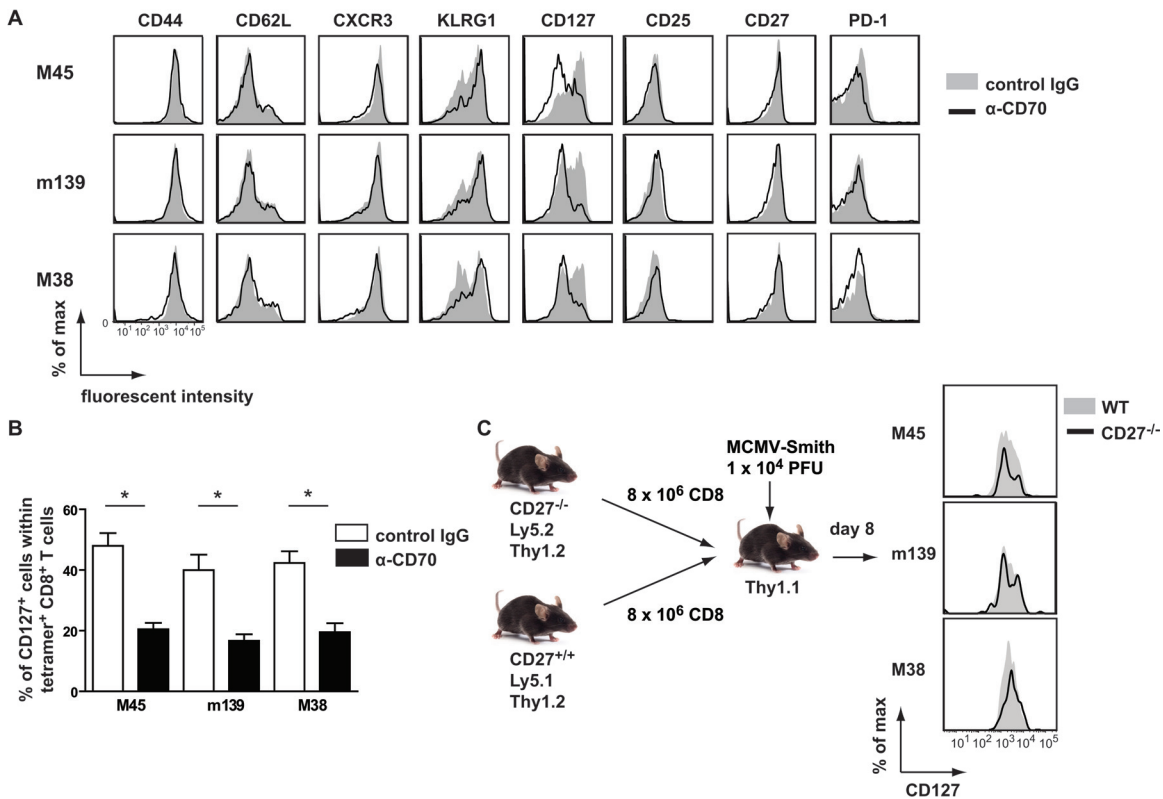

FIG 7 Effects of CD27-CD70 costimulation on the phenotype of MCMV-specific CD8$^+$ T cells. (A) Mice were infected with 1×10^4 PFU MCMV-Smith, and a blocking anti-CD70 or control antibody was administered. At day 8 postinfection, the phenotype of splenic CD8$^+$ T cells was assessed. Representative histogram plots show cell surface expression of the indicated markers on gated MHC class I tetramer-binding CD8$^+$ T cells from anti-CD70 (solid black lines) or control (filled gray histograms) antibody-treated mice. (B) Percentages of tetramer$^+$ CD8$^+$ T cells expressing CD127. Pooled data from two independent experiments are shown as means + SEM. (C) Schematic of experimental setup. CD8$^+$ T cells were isolated from naive CD27$^{-/-}$ Ly5.2 and CD27$^{+/+}$ Ly5.1 mice and transferred 1:1 into naive Thy1.1 recipients, which were subsequently infected with 1×10^4 PFU MCMV-Smith. Representative histograms show CD127 expression on gated tetramer$^+$ CD27$^{-/-}$ Ly5.2 (solid black lines) and CD27$^{+/+}$ Ly5.1 (filled gray histograms) CD8$^+$ T cells at day 8 postinfection. Experiments were performed twice with similar results. For all experiments, statistical significance was determined with the Student t test (*, $P < 0.05$; $n = 3$ to 8).
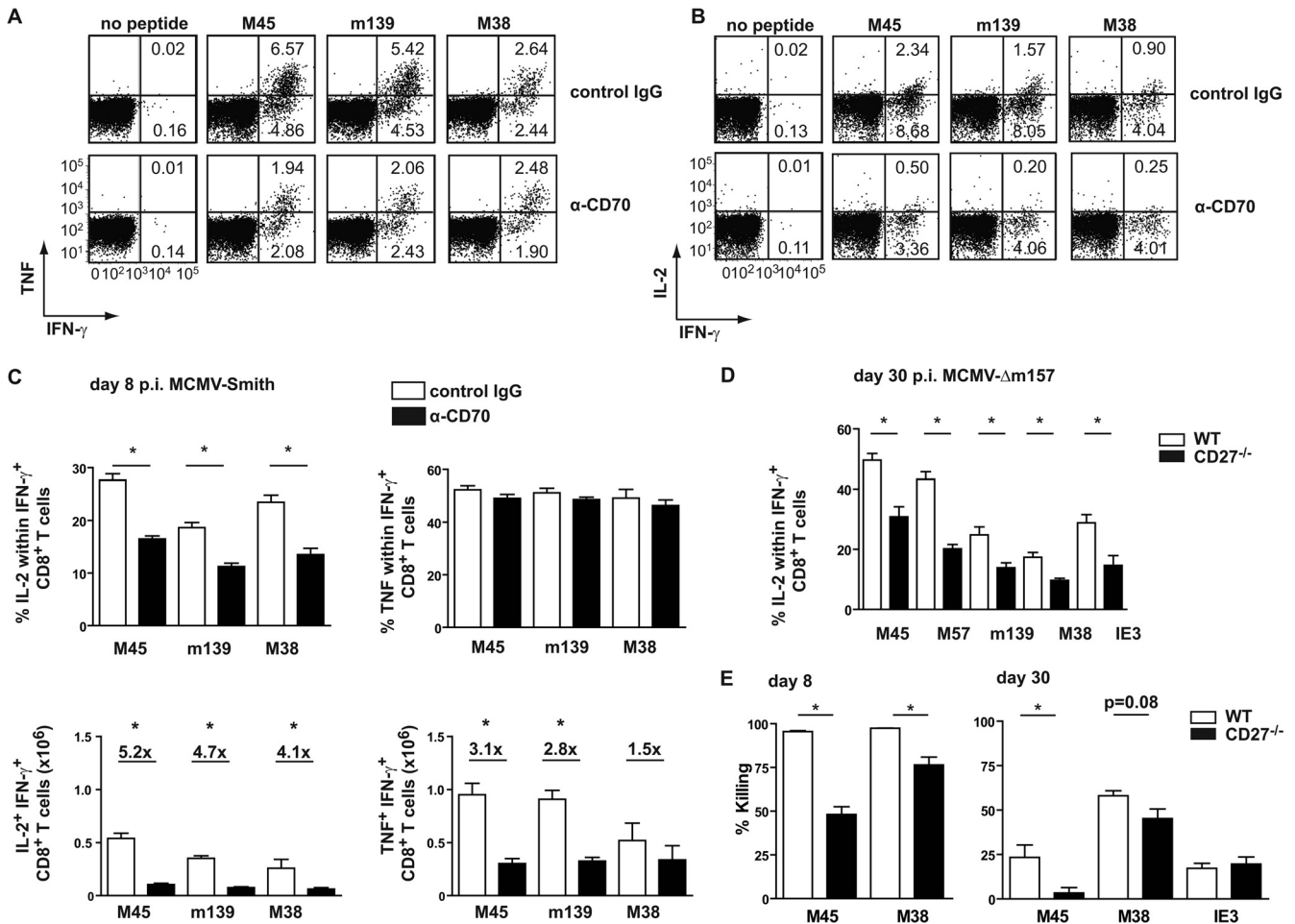
FIG 8 CD27-CD70 costimulation influences autocrine IL-2 production of both noninflationary and inflationary CD8^{+} T cell populations. (A to C) Mice were infected with 1×10^4 PFU MCMV-Smith, and a blocking anti-CD70 or control antibody was administered. At 8 days postinfection, the MCMV-specific CD8^{+} T cell responses in the spleen were analyzed by intracellular cytokine staining upon peptide restimulation. (A) Representative flow cytometry plots showing intracellular TNF and IFN-γ production by splenic CD8^{+} T cells after restimulation with the indicated class I peptides at day 8 postinfection. Percentages of TNF^{+} IFN-γ^{+} and IFN-γ^{+} cells are indicated. (B) Representative flow cytometry plots showing intracellular IL-2 and IFN-γ production by splenic CD8^{+} T cells after restimulation with the indicated class I peptides at day 8 postinfection. Percentages of IL-2^{+} IFN-γ^{+} and IFN-γ^{+} cells are indicated. (C) Percentages of IL-2- or TNF-producing cells within the IFN-γ^{+} CD8^{+} T cells and total numbers of IFN-γ^{+} IL-2^{+} or IFN-γ^{+} TNF^{+} CD8^{+} T cells per spleen. Fold differences are indicated. Pooled data from two independent experiments are shown. (D) Wild-type and CD27^{−/−} mice were infected with 1×10^4 PFU MCMV-Δm157, and at day 30 postinfection, the percentage of IFN-γ^{+} CD8^{+} T cells coproducing IL-2 in the spleen was determined by intracellular cytokine staining. Pooled data from two independent experiments are shown. (E) WT and CD27^{−/−} mice received differentially labeled target cells, at days 8 and 30 postinfection, that were unloaded or loaded with M45, M38, or IE3. The graphs show the percentages of target cells that were killed after 3 h (day 8) or 5 h (day 30). For all experiments, bar graphs show means and SEM. Statistical significance was determined with the Student t test (*, $P < 0.05$; $n = 4$ to 8).

gering on CD8^{+} T cells or due to other mechanisms (e.g., differences in viral load), we performed an adoptive transfer experiment in which both CD27^{+/+} CD8^{+} T cells and CD27^{−/−} CD8^{+} T cells were transferred into the same host, which was subsequently infected with MCMV-Smith (Fig. 7C). We found that the expression levels of CD127 were similar on the adoptively transferred CD27^{−/−} and CD27^{+/+} tetramer^{+} CD8^{+} T cells. Similar results were found when recipient mice were infected with MCMV-Δm157 (data not shown). Together, these results indicate that CD27 signaling does not have a direct effect on the expression of CD127.

CD27 costimulation contributes to autocrine IL-2 production by CMV-specific T cells. To determine whether CD27-CD70 interactions influence the polyfunctional cytokine capacity of CMV-specific T cells, the ability of IFN-γ^{+} CD8^{+} T cells to co-

produce IL-2 and TNF was examined by multicolor intracellular cytokine staining. At day 8 postinfection, the percentages of IFN-γ^{+} CD8^{+} cells coproducing TNF were not influenced by CD70 abrogation, but the percentages of IL-2^{+} cells within noninflationary and inflationary IFN-γ^{+} CD8^{+} T cell populations were severely compromised. Calculation of the total numbers of IFN-γ^{+} CD8^{+} cells coproducing TNF and IL-2 clearly confirmed the selective loss of IL-2-producing cells due to the lack of CD27-CD70 costimulation (Fig. 8A to C). Experiments performed with CD27^{−/−} mice recapitulated these results (data not shown). Additionally, at day 30 postinfection, the IL-2 production of MCMV-specific CD8^{+} T cells was diminished in CD27^{−/−} mice compared to WT mice (Fig. 8D). Blocking of CD27-CD70 interactions at late time points postinfection showed that the IL-2 production was affected mainly when CD70-driven costimulation was abrogated
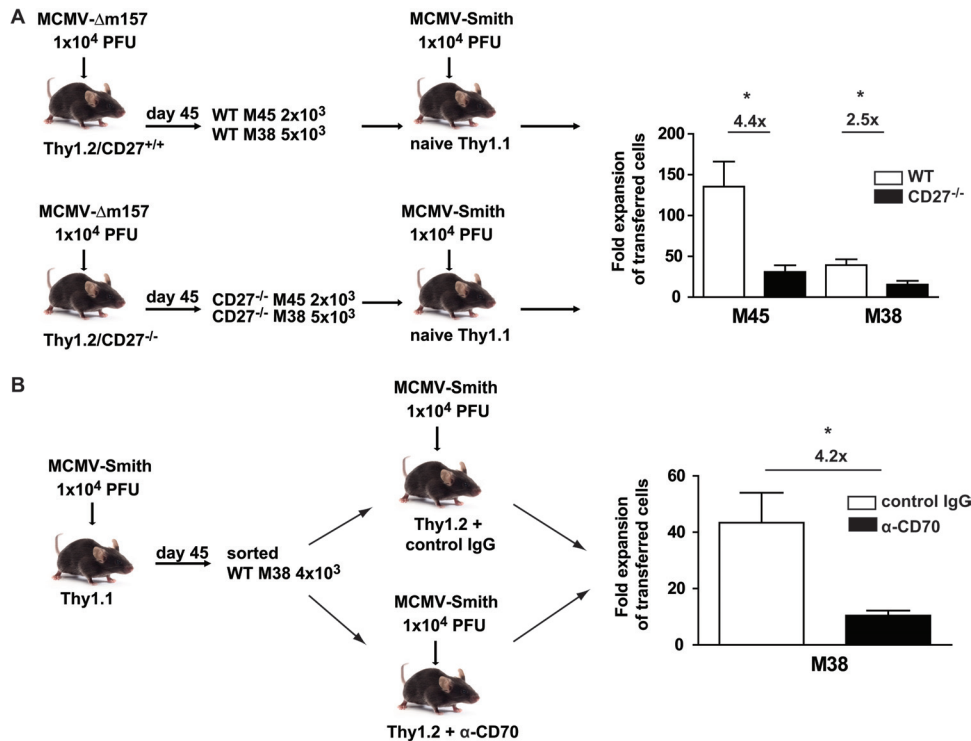
FIG 9 CD27-CD70 costimulation is important for secondary expansion of MCMV-specific CD8$^+$ T cells. (A) WT and CD27$^{-/-}$ mice were infected with 1×10^4 PFU MCMV-Δm157. At day 45 postinfection, M45 and M38 tetramer$^+$ cells were isolated from the spleen and transferred into naive Thy1.1 hosts, which were subsequently infected with 1×10^4 PFU MCMV-Smith. On day 7 after infection, the expansion of donor M45- and M38-specific CD8$^+$ T cells in the spleen was determined by MHC class I tetramer staining. The fold expansion of WT and CD27$^{-/-}$ M45- and M38-specific CD8$^+$ T cells was determined by dividing the absolute numbers of Thy1.2$^+$ tetramer$^+$ CD8$^+$ T cells by the number of cells that were used for the adoptive transfer. Fold differences are indicated. (B) Thy1.1 donor mice were infected with 1×10^4 PFU MCMV-Smith, and at day 45 postinfection, splenic M38 tetramer$^+$ cells were transferred into naive Thy1.2 hosts, which were subsequently infected with 1×10^4 PFU MCMV-Smith. Before and during infection, mice received a blocking anti-CD70 or control antibody. At day 7 postinfection, the fold expansion of M38-specific CD8$^+$ Thy1.1$^+$ T cells was determined. Fold differences are indicated. All bar graphs show means and SEM. Statistical significance was determined by the Student t test (*, $P < 0.05$; $n = 4$).

in the beginning of infection (data not shown). Together, these data show that CD27-CD70 interactions are critical early in CMV infection for the production of autocrine IL-2 by CD8$^+$ T cells throughout infection.

The functional killing capacity of CD8$^+$ T cells at day 8 and day 30 postinfection was assessed by an *in vivo* cytotoxicity assay and showed that target cells pulsed with M45 or M38 peptide-loaded splenocytes were killed less efficiently in CD27$^{-/-}$ mice than in WT mice (Fig. 8E). No differences in the killing of IE3-loaded target cells were found at 30 days postinfection, which is likely linked to the numbers of specific CD8$^+$ T cells.

CD27-CD70 costimulation is important for the secondary expansion of CMV-specific CD8$^+$ T cells. The ability to rapidly respond to a secondary infection is a hallmark of memory T cells (41). In CMV infection, high levels of effector memory T cells are maintained, but nevertheless, adequate reinfection with CMV is possible (11). Adoptive transfer experiments were performed to examine if CD27 costimulation is involved in the secondary expansion of MCMV-specific memory CD8$^+$ T cells. M45- and M38-specific CD8$^+$ T cells were isolated from persistently MCMV-infected CD27$^{+/+}$ or CD27$^{-/-}$ mice, and equivalent numbers of CD27-proficient or -deficient cells were transferred into naive congenic Thy1.1 host mice, which were subsequently infected with MCMV-Smith. The secondary expansion of M45-specific CD27$^{-/-}$ CD8$^+$ T cells was reduced 4.4-fold in compari-

son with that of CD27-proficient cells. The expansion of CD27$^{-/-}$ M38-specific T cells was also reduced, albeit to a lesser extent (~2.5-fold) (Fig. 9A). In addition, CD27$^{-/-}$ but not WT TCR transgenic OT-I cells failed to expand after reinfection with MCMV-OVA 6 months after primary infection (data not shown). These results show that secondary CD8$^+$ T cell expansion is dependent on CD27, which is consistent with other reports (22, 42, 43).

To examine the influence of a potential "programming" effect of CD27 in the priming phase on the capacity to divide upon rechallenge, additional adoptive transfer experiments were performed. M38-specific CD8$^+$ T cells were isolated from latently infected Thy1.1 donor mice and transferred into Thy1.2 hosts that were treated with either anti-CD70 or control antibody. All recipient mice were subsequently infected with MCMV-Smith. At 7 days postinfection, the M38-specific CD8$^+$ T cell response in control antibody-treated mice was increased compared to that in mice with abrogated CD27-CD70 interactions (Fig. 9B). Together, these data show that CD27-CD70 costimulation is important throughout infection and during rechallenge for the secondary expansion of MCMV-specific CD8$^+$ T cells.

DISCUSSION

CD27 expression is commonly used as an important marker for lymphocyte subsets, and the loss of CD27 on circulating T cells
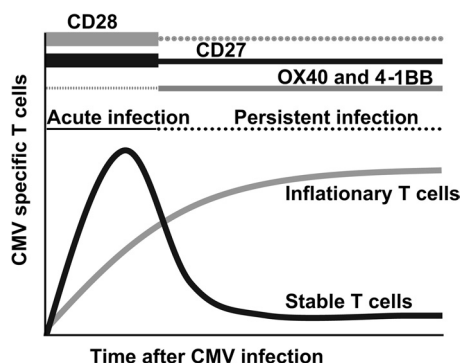
FIG 10 Model for the role of costimulatory molecules in the development of CMV-specific T cell immunity. T cell costimulation is important for the development of MCMV-specific inflationary and noninflationary T cell responses. Whereas CD28-B7 costimulatory interactions are important predominantly during the acute phase of infection, 4-1BB- and OX40-mediated costimulation is important for memory T cell inflation during the persistent phase. CD27-CD70 costimulation is important for both inflationary and noninflationary T cell responses during the course of acute and persistent infections.

seems to be associated uniquely with HCMV seropositivity (20). By using a relevant experimental CMV model, we underscore this finding and further show that CD27 loss occurs specifically on inflationary memory T cells and is not dependent on interaction with its ligand, CD70. During acute infection, CD27-CD70 costimulation enhances the expansion of MCMV-specific CD4$^+$ and CD8$^+$ T cells, likely related to direct effects on cell division and survival (44–46). Moreover, CD27-CD70 interactions are required for both the establishment of MCMV-specific stable memory T cell pools and the accumulation of inflationary T cells. The finding that the secondary expansion of CMV-specific T cells was also compromised by the lack of CD27-CD70 costimulation during priming and rechallenge underlines the importance of this costimulatory receptor-ligand pair against recurrent infections.

Differential requirements of costimulatory molecules for the generation of CMV-specific memory T cell pools have been reported. Interactions between CD28, expressed on naive T cells, and its ligands B7.1 (CD80) and B7.2 (CD86) are not strictly required for memory T cell inflation but are important for primary T cell expansion and the development of stable memory pools (28, 29). In contrast, the costimulatory TNF receptor (TNFR) family members 4-1BB and OX40, which are upregulated on T cells upon TCR triggering, contribute predominantly to the accumulation of inflationary T cells during the persistent phase (47, 48). This indicates a spatiotemporal disparity between the requirements for different costimulatory signals and places CD27, as an important molecule during both acute and persistent infections, in a prominent role for the development of CMV-specific T cell immunity (see the model depicted in Fig. 10).

The current view is that inflationary T cells are continuously exposed to low levels of viral antigens presented by latently infected nonhematopoietic cells (15, 49–51). The downmodulation of CD27 is most likely also related to such repeated antigenic stimulation. Supporting this notion is the observation that in patients who shed HCMV in the urine for extended periods, which indicates an active infection, increased frequencies of circulating CD27$^-$ CD8$^+$ T cells are found compared to those of patients with HCMV-negative urine cultures (52). The particular loss of CD27

expression during persistent MCMV infection on inflationary rather than noninflationary memory CD8$^+$ T cells raises the question of whether this also occurs during HCMV infection.

Consistent with the results from Peperzak et al. (53), we found diminished autocrine IL-2 production when CD27-CD70 interactions were abrogated. Whether this decrease in autocrine IL-2 production by T cells is instructed exclusively by CD27 or other (co)stimulatory signals which also influence IL-2 production (29), such as CD28, are (partly) complementary or redundant remains to be elucidated. The recent finding that autocrine IL-2 production is critical for the secondary expansion of memory CD8$^+$ T cells (54) indicates that the observed reduced IL-2 production of CD27$^{-/-}$ memory T cells might be involved in the reduced secondary expansion of these cells upon reinfection with CMV. In this respect, it is interesting that inflationary T cells produce less autocrine IL-2 than stable memory T cells (14), consistent with the fold difference observed in secondary expansion between stable and inflationary T cells.

During acute infections caused by vesicular stomatitis virus, vaccinia virus, and *Listeria monocytogenes*, the primary expansion of CD8$^+$ T cell responses depends on CD27-CD70 interactions (55), whereas depending on the strain of influenza virus, a contribution of CD27-CD70 interactions to T cell expansion was observed during rechallenge and, to a lesser extent, during primary acute infection (22, 34). Furthermore, highly virulent vaccinia virus strains that engage CD27 elicit large numbers of protective memory CD8$^+$ T cells, whereas strains exhibiting reduced virulence do not employ CD27 and elicit a weak memory CD8$^+$ T cell response (56). During chronic LCMV infection, effects of CD27-CD70 costimulation can, however, result in detrimental effects on adaptive immunity (57–59). In this respect, it is interesting that in a transgenic mouse model of constitutive CD27 triggering (60), progressive effector T cell formation occurs, which is accelerated by the absence of CD95-mediated T cell death (61) and eventually results in a lethal immunodeficiency (62). The current study shows that during CMV infection, considered a low-level persistent infection, CD27 has a valuable impact on both the primary and secondary expansion of virus-specific T cells. Thus, CD27-CD70 interactions are highly beneficial during acute and low-level persistent infections, but during highly active chronic infections, stimulation of this costimulatory pathway may lead to an unfavorable outcome with respect to T cell immunity.

In summary, we show that CD27-CD70 costimulatory signals are crucial for the development of both noninflationary and inflationary T cell pools during acute and persistent infections. Targeting this costimulatory pathway could be beneficial to advance cellular immunotherapy in individuals suffering from severe HCMV disease. Furthermore, due to the high frequency of CMV-specific (inflationary) effector memory T cells throughout infection, CMV is an interesting candidate to exploit as a vaccine vector. CMV-based vectors containing simian immunodeficiency virus (SIV) proteins have been used successfully in macaque studies, with the vaccinated macaques showing enhanced viral control upon SIV challenge and protection from severe disease for a prolonged period (63). The efficacy of such CMV-based vaccines might be improved by targeting CD27-CD70 costimulation, given its role in the maintenance of inflationary effector memory pools.

ACKNOWLEDGMENTS

REFERENCES

1. **Alcami A, Koszinowski UH.** 2000. Viral mechanisms of immune evasion. Immunol. Today **21:**447–455.

2. **Mocarski ES, Jr.** 2002. Immunomodulation by cytomegaloviruses: manipulative strategies beyond evasion. Trends Microbiol. **10:**332–339.

3. **Cannon MJ, Schmid DS, Hyde TB.** 2010. Review of cytomegalovirus seroprevalence and demographic characteristics associated with infection. Rev. Med. Virol. **20:**202–213.

4. **Pereira L, Maidji E, McDonagh S, Tabata T.** 2005. Insights into viral transmission at the uterine-placental interface. Trends Microbiol. **13:** 164–174.

5. **Riddell SR, Greenberg PD.** 1997. T cell therapy of human CMV and EBV infection in immunocompromised hosts. Rev. Med. Virol. **7:**181–192.

6. **Gamadia LE, Remmerswaal EB, Weel JF, Bemelman F, van Lier RA, ten Berge IJ.** 2003. Primary immune responses to human CMV: a critical role for IFN-gamma-producing CD4+ T cells in protection against CMV disease. Blood **101:**2686–2692.

7. **Reddehase MJ, Weiland F, Munch K, Jonjic S, Luske A, Koszinowski UH.** 1985. Interstitial murine cytomegalovirus pneumonia after irradiation: characterization of cells that limit viral replication during established infection of the lungs. J. Virol. **55:**264–273.

8. **Reddehase MJ, Mutter W, Munch K, Buhring HJ, Koszinowski UH.** 1987. CD8-positive T lymphocytes specific for murine cytomegalovirus immediate-early antigens mediate protective immunity. J. Virol. **61:**3102–3108.

9. **Reddehase MJ, Jonjic S, Weiland F, Mutter W, Koszinowski UH.** 1988. Adoptive immunotherapy of murine cytomegalovirus adrenalitis in the immunocompromised host: CD4-helper-independent antiviral function of CD8-positive memory T lymphocytes derived from latently infected donors. J. Virol. **62:**1061–1065.

10. **Jonjic S, Mutter W, Weiland F, Reddehase MJ, Koszinowski UH.** 1989. Site-restricted persistent cytomegalovirus infection after selective long-term depletion of CD4+ T lymphocytes. J. Exp. Med. **169:**1199–1212.

11. **Hansen SG, Powers CJ, Richards R, Ventura AB, Ford JC, Siess D, Axthelm MK, Nelson JA, Jarvis MA, Picker LJ, Fruh K.** 2010. Evasion of CD8+ T cells is critical for superinfection by cytomegalovirus. Science **328:**102–106.

12. **Walter EA, Greenberg PD, Gilbert MJ, Finch RJ, Watanabe KS, Thomas ED, Riddell SR.** 1995. Reconstitution of cellular immunity against cytomegalovirus in recipients of allogeneic bone marrow by transfer of T-cell clones from the donor. N. Engl. J. Med. **333:**1038–1044.

13. **Snyder CM, Cho KS, Bonnett EL, van Shellam DSGR, Hill AB.** 2008. Memory inflation during chronic viral infection is maintained by continuous production of short-lived, functional T cells. Immunity **29:**650–659.

14. **Munks MW, Cho KS, Pinto AK, Sierro S, Klenerman P, Hill AB.** 2006. Four distinct patterns of memory CD8 T cell responses to chronic murine cytomegalovirus infection. J. Immunol. **177:**450–458.

15. **O'Hara GA, Welten SP, Klenerman P, Arens R.** 2012. Memory T cell inflation: understanding cause and effect. Trends Immunol. **33:**84–90.

16. **Arens R, Wang P, Sidney J, Loewendorf A, Sette A, Schoenberger SP, Peters B, Benedict CA.** 2008. Cutting edge: murine cytomegalovirus induces a polyfunctional CD4 T cell response. J. Immunol. **180:**6472–6476.

17. **Appay V, Dunbar PR, Callan M, Klenerman P, Gillespie GM, Papagno L, Ogg GS, King A, Lechner F, Spina CA, Little S, Havlir DV, Richman DD, Gruener N, Pape G, Waters A, Easterbrook P, Salio M, Cerundolo V, McMichael AJ, Rowland-Jones SL.** 2002. Memory CD8+ T cells vary in differentiation phenotype in different persistent virus infections. Nat. Med. **8:**379–385.

18. **Kuijpers TW, Vossen MT, Gent MR, Davin JC, Roos MT, Wertheim-van Dillen PM, Weel JF, Baars PA, van Lier RA.** 2003. Frequencies of circulating cytolytic, CD45RA+CD27−, CD8+ T lymphocytes depend on infection with CMV. J. Immunol. **170:**4342–4348.

19. **Gamadia LE, van Leeuwen EM, Remmerswaal EB, Yong SL, Surachno S, Wertheim-van Dillen PM, ten Berge IJ, van Lier RA.** 2004. The size

20. **van Lier RA, ten Berge IJ, Gamadia LE.** 2003. Human CD8(+) T-cell differentiation in response to viruses. Nat. Rev. Immunol. **3:**931–939.

21. **Sierro S, Rothkopf R, Klenerman P.** 2005. Evolution of diverse antiviral CD8+ T cell populations after murine cytomegalovirus infection. Eur. J. Immunol. **35:**1113–1123.

22. **Hendriks J, Gravestein LA, Tesselaar K, van Lier RA, Schumacher TN, Borst J.** 2000. CD27 is required for generation and long-term maintenance of T cell immunity. Nat. Immunol. **1:**433–440.

23. **Coquet JM, Middendorp S, van der Horst G, Kind J, Veraar EA, Xiao Y, Jacobs H, Borst J.** 2013. The CD27 and CD70 costimulatory pathway inhibits effector function of T helper 17 cells and attenuates associated autoimmunity. Immunity **38:**53–65.

24. **Council of Europe.** 1986. Guidelines on the protection of experimental animals. Council of Europe, Brussels, Belgium.

25. **Schneider K, Loewendorf A, De TC, Fulton J, Rhode A, Shumway H, Ha S, Patterson G, Pfeffer K, Nedospasov SA, Ware CF, Benedict CA.** 2008. Lymphotoxin-mediated crosstalk between B cells and splenic stroma promotes the initial type I interferon response to cytomegalovirus. Cell Host Microbe **3:**67–76.

26. **Bubic I, Wagner M, Krmpotic A, Saulig T, Kim S, Yokoyama WM, Jonjic S, Koszinowski UH.** 2004. Gain of virulence caused by loss of a gene in murine cytomegalovirus. J. Virol. **78:**7536–7544.

27. **Ahmed R, Salmi A, Butler LD, Chiller JM, Oldstone MB.** 1984. Selection of genetic variants of lymphocytic choriomeningitis virus in spleens of persistently infected mice. Role in suppression of cytotoxic T lymphocyte response and viral persistence. J. Exp. Med. **160:**521–540.

28. **Arens R, Loewendorf A, Her MJ, Schneider-Ohrum K, Shellam GR, Janssen E, Ware CF, Schoenberger SP, Benedict CA.** 2011. B7-mediated costimulation of CD4 T cells constrains cytomegalovirus persistence. J. Virol. **85:**390–396.

29. **Arens R, Loewendorf A, Redeker A, Sierro S, Boon L, Klenerman P, Benedict CA, Schoenberger SP.** 2011. Differential B7-CD28 costimulatory requirements for stable and inflationary mouse cytomegalovirus-specific memory CD8 T cell populations. J. Immunol. **186:**3874–3881.

30. **Altman JD, Moss PA, Goulder PJ, Barouch DH, McHeyzer-Williams MG, Bell JI, McMichael AJ, Davis MM.** 1996. Phenotypic analysis of antigen-specific T lymphocytes. Science **274:**94–96.

31. **Matloubian M, Somasundaram T, Kolhekar SR, Selvakumar R, Ahmed R.** 1990. Genetic basis of viral persistence: single amino acid change in the viral glycoprotein affects ability of lymphocytic choriomeningitis virus to persist in adult mice. J. Exp. Med. **172:**1043–1048.

32. **Oshima H, Nakano H, Nohara C, Kobata T, Nakajima A, Jenkins NA, Gilbert DJ, Copeland NG, Muto T, Yagita H, Okumura K.** 1998. Characterization of murine CD70 by molecular cloning and mAb. Int. Immunol. **10:**517–526.

33. **Walton SM, Mandaric S, Torti N, Zimmermann A, Hengel H, Oxenius A.** 2011. Absence of cross-presenting cells in the salivary gland and viral immune evasion confine cytomegalovirus immune control to effector CD4 T cells. PLoS Pathog. 7:e1002214. doi:10.1371/journal.ppat.1002214.

34. **van Gisbergen KP, Klarenbeek PL, Kragten NA, Unger PP, Nieuwenhuis MB, Wensveen FM, ten Tak BAPP, Eldering E, Nolte MA, van Lier RA.** 2011. The costimulatory molecule CD27 maintains clonally diverse CD8(+) T cell responses of low antigen affinity to protect against viral variants. Immunity **35:**97–108.

35. **Arase H, Mocarski ES, Campbell AE, Hill AB, Lanier LL.** 2002. Direct recognition of cytomegalovirus by activating and inhibitory NK cell receptors. Science **296:**1323–1326.

36. **De Colvenaer V, Taveirne S, Delforche M, De Smedt M, Vandekerckhove B, Taghon T, Boon L, Plum J, Leclercq G.** 2011. CD27-deficient mice show normal NK-cell differentiation but impaired function upon stimulation. Immunol. Cell Biol. **89:**803–811.

37. **Jordan S, Krause J, Prager A, Mitrovic M, Jonjic S, Koszinowski UH, Adler B.** 2011. Virus progeny of murine cytomegalovirus bacterial artificial chromosome pSM3fr show reduced growth in salivary glands due to a fixed mutation of MCK-2. J. Virol. **85:**10346–10353.

38. **Hintzen RQ, Lens SM, Beckmann MP, Goodwin RG, Lynch D, van Lier RA.** 1994. Characterization of the human CD27 ligand, a novel member of the TNF gene family. J. Immunol. **152:**1762–1773.

39. **Baars PA, Sierro S, Arens R, Tesselaar K, Hooibrink B, Klenerman P,**

van Lier RA. 2005. Properties of murine (CD8+) CD27− T cells. Eur. J. Immunol. **35**:3131–3141.

40. **Arens R, Schepers K, Nolte MA, van Oosterwijk MF, van Lier RA, Schumacher TN, van Oers MH.** 2004. Tumor rejection induced by CD70-mediated quantitative and qualitative effects on effector CD8+ T cell formation. J. Exp. Med. **199**:1595–1605.

41. **Arens R, Schoenberger SP.** 2010. Plasticity in programming of effector and memory CD8 T-cell formation. Immunol. Rev. **235**:190–205.

42. **Feau S, Garcia Z, Arens R, Yagita H, Borst J, Schoenberger SP.** 2012. The CD4(+) T-cell help signal is transmitted from APC to CD8(+) T-cells via CD27-CD70 interactions. Nat. Commun. **3**:948.

43. **Hendriks J, Xiao Y, Rossen JW, van der Sluijs KF, Sugamura K, Ishii N, Borst J.** 2005. During viral infection of the respiratory tract, CD27, 4-1BB, and OX40 collectively determine formation of CD8+ memory T cells and their capacity for secondary expansion. J. Immunol. **175**:1665–1676.

44. **Hendriks J, Xiao Y, Borst J.** 2003. CD27 promotes survival of activated T cells and complements CD28 in generation and establishment of the effector T cell pool. J. Exp. Med. **198**:1369–1380.

45. **Peperzak V, Veraar EA, Keller AM, Xiao Y, Borst J.** 2010. The Pim kinase pathway contributes to survival signaling in primed CD8+ T cells upon CD27 costimulation. J. Immunol. **185**:6670–6678.

46. **van Oosterwijk MF, Juwana H, Arens R, Tesselaar K, van Oers MH, Eldering E, van Lier RA.** 2007. CD27-CD70 interactions sensitise naive CD4+ T cells for IL-12-induced Th1 cell development. Int. Immunol. **19**:713–718.

47. **Humphreys IR, Loewendorf A, de Trez C, Schneider K, Benedict CA, Munks MW, Ware CF, Croft M.** 2007. OX40 costimulation promotes persistence of cytomegalovirus-specific CD8 T cells: a CD4-dependent mechanism. J. Immunol. **179**:2195–2202.

48. **Humphreys IR, Lee SW, Jones M, Loewendorf A, Gostick E, Price DA, Benedict CA, Ware CF, Croft M.** 2010. Biphasic role of 4-1BB in the regulation of mouse cytomegalovirus-specific CD8(+) T cells. Eur. J. Immunol. **40**:2762–2768.

49. **Seckert CK, Schader SI, Ebert S, Thomas D, Freitag K, Renzaho A, Podlech J, Reddehase MJ, Holtappels R.** 2011. Antigen-presenting cells of haematopoietic origin prime cytomegalovirus-specific CD8 T-cells but are not sufficient for driving memory inflation during viral latency. J. Gen. Virol. **92**:1994–2005.

50. **Simon CO, Holtappels R, Tervo HM, Bohm V, Daubner T, Oehrlein-Karpi SA, Kuhnapfel B, Renzaho A, Strand D, Podlech J, Reddehase MJ, Grzimek NK.** 2006. CD8 T cells control cytomegalovirus latency by epitope-specific sensing of transcriptional reactivation. J. Virol. **80**:10436–10456.

51. **Torti N, Walton SM, Brocker T, Rulicke T, Oxenius A.** 2011. Non-hematopoietic cells in lymph nodes drive memory CD8 T cell inflation during murine cytomegalovirus infection. PLoS Pathog. **7**:e1002313. doi: 10.1371/journal.ppat.1002313.

52. **Gamadia LE, Rentenaar RJ, Baars PA, Remmerswaal EB, Surachno S, Weel JF, Toebes M, Schumacher TN, ten Berge IJ, van Lier RA.** 2001. Differentiation of cytomegalovirus-specific CD8(+) T cells in healthy and immunosuppressed virus carriers. Blood **98**:754–761.

53. **Peperzak V, Xiao Y, Veraar EA, Borst J.** 2010. CD27 sustains survival of CTLs in virus-infected nonlymphoid tissue in mice by inducing autocrine IL-2 production. J. Clin. Invest. **120**:168–178.

54. **Feau S, Arens R, Togher S, Schoenberger SP.** 2011. Autocrine IL-2 is required for secondary population expansion of CD8(+) memory T cells. Nat. Immunol. **12**:908–913.

55. **Schildknecht A, Miescher I, Yagita H, van den Broek M.** 2007. Priming of CD8+ T cell responses by pathogens typically depends on CD70-mediated interactions with dendritic cells. Eur. J. Immunol. **37**:716–728.

56. **Salek-Ardakani S, Flynn R, Arens R, Yagita H, Smith GL, Borst J, Schoenberger SP, Croft M.** 2011. The TNFR family members OX40 and CD27 link viral virulence to protective T cell vaccines in mice. J. Clin. Invest. **121**:296–307.

57. **Matter M, Mumprecht S, Pinschewer DD, Pavelic V, Yagita H, Krautwald S, Borst J, Ochsenbein AF.** 2005. Virus-induced polyclonal B cell activation improves protective CTL memory via retained CD27 expression on memory CTL. Eur. J. Immunol. **35**:3229–3239.

58. **Matter M, Odermatt B, Yagita H, Nuoffer JM, Ochsenbein AF.** 2006. Elimination of chronic viral infection by blocking CD27 signaling. J. Exp. Med. **203**:2145–2155.

59. **Penaloza-Macmaster P, Rasheed AU, Iyer SS, Yagita H, Blazar BR, Ahmed R.** 2011. Opposing effects of CD70 costimulation during acute and chronic lymphocytic choriomeningitis virus infection of mice. J. Virol. **85**:6168–6174.

60. **Arens R, Tesselaar K, Baars PA, van Schijndel GM, Hendriks J, Pals ST, Krimpenfort P, Borst J, van Oers MH, van Lier RA.** 2001. Constitutive CD27/CD70 interaction induces expansion of effector-type T cells and results in IFNgamma-mediated B cell depletion. Immunity **15**:801–812.

61. **Arens R, Baars PA, Jak M, Tesselaar K, van der Valk M, van Oers MH, van Lier RA.** 2005. Cutting edge: CD95 maintains effector T cell homeostasis in chronic immune activation. J. Immunol. **174**:5915–5920.

62. **Tesselaar K, Arens R, van Schijndel GM, Baars PA, van der Valk MA, Borst J, van Oers MH, van Lier RA.** 2003. Lethal T cell immunodeficiency induced by chronic costimulation via CD27-CD70 interactions. Nat. Immunol. **4**:49–54.

63. **Hansen SG, Ford JC, Lewis MS, Ventura AB, Hughes CM, Coyne-Johnson L, Whizin N, Oswald K, Shoemaker R, Swanson T, Legasse AW, Chiuchiolo MJ, Parks CL, Axthelm MK, Nelson JA, Jarvis MA, Piatak M, Jr, Lifson JD, Picker LJ.** 2011. Profound early control of highly pathogenic SIV by an effector memory T-cell vaccine. Nature **473**:523–527.